Acta Crystallographica Section B
Structural Science
ISSN 0108-7681

X-ray investigations of sulfur-containing fungicides. III. Intramolecular forces governing the conformation of a novel orthorhombic polymorph of benzoylmethyl phenyl sulfone, benzoylmethyl 4-chlorophenyl sulfone and benzoylphenylmethyl phenyl sulfone

W. M. Wolf

Institute of General and Ecological Chemistry (I-17), Technical University of Łód Żwirki 36, 90-924 Łódź, Poland

Correspondence e-mail: wmwolf@p.lodz.pl

Received 17 May 2001
Accepted 2 October 2001

Part II: see Wolf (2001).

The crystal and molecular structures of three β-ketosulfones: benzoylmethyl phenyl sulfone (I), benzoylmethyl 4-chlorophenyl sulfone (II) and benzoylphenylmethyl phenyl sulfone (III) have been investigated using X-ray analysis and quantum mechanics *ab initio* calculations. Compound (I) crystallizes in the monoclinic and orthorhombic crystal systems. The crystal structure of the orthorhombic polymorph has not been reported previously. At room temperature and in the presence of daylight the pale yellow orthorhombic crystals undergo transformation to the stable colourless monoclinic polymorph. Hyperconjugative σ(S—C1) $-$ π^*(C2═O3) and σ^*(S—C1) $-$ π(C2═O3) stabilization energies in benzoylmethyl phenyl sulfones are highly dependent on the central dihedral angle α: S—C1—C2═O3 and are largest for a *gauche* arrangement, as found in both crystal forms of (I). The electron density distribution in all compounds (I), (II) and (III) is significantly affected by interactions of oxygen lone pairs with non-bonding orbitals of the adjacent S—C1 and C1—C2 bonds. The latter effect is responsible for back-donation of the electron density from O atoms towards the central part of the molecule.

1. Introduction

Various derivatives of α-unsubstituted benzoylmethyl phenyl sulfone have been studied quite intensively over the past years (Grossert *et al.*, 1988; Kokkou & Cheer, 1986; Krawiec *et al.*, 1989; Dal Colle *et al.*, 1995; Distefano *et al.*, 1996; Gałdecka & Gałdecki, 1999). In these compounds two strongly electron-withdrawing, phenylsulfonyl and benzoyl moieties are separated by a methylene group. Photoelectron, NMR and IR spectroscopy supported by X-ray crystallography and *ab initio* quantum mechanics calculations showed that the conformation of β-ketosulfones and β-ketosulfoxides is strongly influenced by two cross donor–acceptor interactions existing between pairs of the sulfonyl or sulfinyl S═O and β-carbonyl C═O dipoles. These interactions back-donate electron density from the highly negative O atoms towards the sulfur and β-C atoms bearing large positive charge (Distefano *et al.*, 1991; Olivato *et al.*, 1998, 2000). Dal Colle *et al.* (1995) argued that these stereoelectronic interactions prompt the S—C$_\alpha$ bond to be positioned *gauche* with respect to the β-carbonyl double bond. Indeed, most of the X-ray determined structures of α,α-unsubstituted β-ketosulfones exist in a *gauche* conformation (Allen & Kennard, 1993).

The α,α-unsubstituted derivatives of benzoylmethyl phenyl sulfone are examples of molecular systems with the easily

dissociating methylene acidic C—H bonds (Amel & Marek, 1973). The resulting carbanions are stabilized by the electron density transfers to the neighbouring highly positive sulfur and β-C atoms. The NMR chemical proton shifts of the α-methylene H atoms are very sensitive to the electron density changes of their parent C atoms and were used to study the transmission of the substituent effect through the sulfonyl and β-carbonyl groups (Borchardt, Kopkowski, Kornacki & Zakrzewski, 1990).

Biological tests have shown that the benzoylmethyl phenyl sulfone and its derivatives effectively inhibit the growth of *Aphanomyces cochlioides* and *Rhisoctonia solani* (Drabik *et al.*, 1990; Borchardt, Kopkowski, Wasilewski & Zakrzewski, 1990). In particular, fungicidal activity is increased after exposing samples containing fungi colonies with added fungicide to radiation of daylight characteristics (Zakrzewski & Kacała, 1998; Zakrzewski, 1999). Wagner & Lindstrom (1987) have shown that β-ketosulfones undergo relatively slow excited radical cleavage to generate α-keto radicals and sulfur-centred radicals. Products of this gradual photodynamic degradation can steadily penetrate the cell walls of fungi colonies and secure destruction of the mycelium over a longer period of time. The present work is part of a project aimed at identification of molecular properties which are responsible for the antimycotic activity of the selected β-ketosulfones (Wolf, 1999*a*,*b*, 2000, 2001).

In this paper the main intramolecular interactions which stabilize the conformation of benzoylmethyl phenyl sulfone (I) and two novel β-ketosulfones: benzoylmethyl 4-chlorophenyl sulfone (II) and benzoylphenylmethyl phenyl sulfone (III) are described.

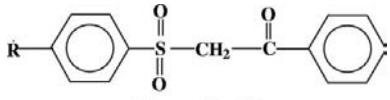

(I) R = H
(II) R = Cl

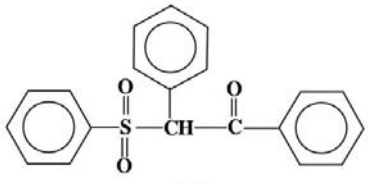

(III)

Their crystal structures have been determined by X-ray analysis. The benzoylmethyl phenyl sulfone crystallizes in either the monoclinic or the orthorhombic crystal system. X-ray structure determinations of the stable, monoclinic polymorph (space group $P2_1/c$) have been reported twice so far (Krawiec *et al.*, 1989; Dal Colle *et al.*, 1995). At room temperature the pale yellow, fragile orthorhombic crystals undergo transformation to the colourless monoclinic form. Both polymorphs were characterized by single-crystal X-ray analysis. To the best of my knowledge, this is the first report on a polymorphic transformation of β-ketosulfone. Electronic properties of the investigated molecules were calculated at the *ab initio* molecular orbital level using the density functional theory and the restricted Hartree–Fock methodologies. Molecular stabilization energies resulting from hyperconjugative interactions were calculated using the Weinhold's and co-workers natural bond orbitals approach (Reed *et al.*, 1988).

2. Experimental

2.1. Preparation

All investigated compounds were synthesized by Dr A. Zakrzewski at the Department of Technology and Chemical Engineering, Technical and Agricultural Academy, Bydgoszcz, Poland. (I), (II) and (III) were obtained by condensation of the sodium benzenesulfinate with phenacyl bromide, *p*-chlorophenacyl bromide and desyl chloride, respectively. Reactions were carried out in tetrahydrofuran and in the presence of tetra-*n*-butylammonium bromide (Borchardt, Kopkowski, Wasilewski & Zakrzewski, 1990).

2.2. Crystallization and X-ray structure analysis

Good quality crystals were obtained by vapour diffusion. Samples of the compounds were dissolved in a 2:1 mixture of chloroform and 2-propanol and equilibrated against the pure 2-propanol for approximately 1 week. All crystallizations were performed in darkness at room temperature. Under these conditions benzoylmethyl phenyl sulfone (I) crystallizes in the orthorhombic system (space group: $P2_12_12_1$) giving pale yellow crystals. This polymorph is named hereafter as (Io). Interestingly, when the freshly obtained long pale yellow prisms of (Io) were left at room temperature in the presence of daylight for $\sim$2 weeks they underwent a polymorphic transformation yielding the colourless stable crystals of the well known monoclinic form, named hereafter as (Im). Both polymorphs have been unequivocally identified by X-ray structure analysis using the same monocrystal before and after the conversion. In order to stabilize the fragile orthorhombic crystal, the X-ray data of (Io) were collected at 110 K. The Oxford Cryosystem cooling device mounted on the Kuma Diffraction KM-4 diffractometer was used. Significant decay (20%) of the diffracting power of (II) reflects its photodynamic instability resulting in a completeness of the data set of only 82%. No polymorphic transformation similar to that one observed in (Io) was detected in the crystal.

Details of crystal symmetry, data collections, structure determinations and refinements are summarized in Table 1.[2] All non-H atoms were localized on *E* maps. The H atoms of all structures were routinely located in difference Fourier maps calculated after three cycles of an anisotropic refinement. Their positional and isotropic displacement parameters were allowed to refine freely. In (Io) three reflections: $\bar{1}$,1,31; $\bar{2}$,1,31; $\bar{2}$,1,32; and in (II) four reflections: 3,0,2; 4,3,3; 4,3,1; 3,2,2; all identified as outliers, were not used in the final refinement. Correct chirality of the crystal of (Io) has been assigned by

[2] Supplementary data for this paper are available from the IUCr electronic archives (Reference: OS0077). Services for accessing these data are described at the back of the journal.

Table 1
Experimental details.

	(Io)	(Im)	(II)	(III)
Crystal data				
Chemical formula	$C_{14}H_{12}O_3S$	$C_{14}H_{12}O_3S$	$C_{14}H_{11}ClO_3S$	$C_{20}H_{16}O_3S$
Chemical formula weight	260.3	260.3	294.74	336.39
Cell setting, space group	Orthorhombic, $P2_12_12_1$	Monoclinic, $P2_1/c$	Orthorhombic, $Pbca$	Monoclinic, $P2_1/c$
a, b, c (Å)	4.8177 (7), 9.4100 (12), 26.719 (3)	9.2145 (9), 5.3594 (6), 25.665 (3)	13.469 (1), 7.4580 (1), 26.656 (2)	9.1282 (8), 17.2532 (19), 10.8670 (11)
β (°)	90	98.448 (9)	90	105.794 (7)
V (Å^3)	1211.3 (3)	1253.7 (2)	2677.6 (9)	1646.8 (3)
Z	4	4	8	4
D_x (Mg m^{-3})	1.427	1.379	1.462	1.357
Radiation type	Mo $K\alpha$	Mo $K\alpha$	Cu $K\alpha$	Mo $K\alpha$
No. of reflections for cell parameters	50	43	60	48
θ range (°)	5–16	4.6–14.0	6–18	4.1–17.0
μ (mm^{-1})	0.264	0.255	4.000	0.211
Temperature (K)	110 (1)	290 (2)	290 (2)	290 (2)
Crystal form, colour	Plate, pale yellow	Plate, colourless	Needle, colourless	Prism, colourless
Crystal size (mm)	0.6 × 0.4 × 0.2	0.6 × 0.4 × 0.2	0.50 × 0.20 × 0.15	0.5 × 0.4 × 0.3
Data collection				
Diffractometer	Kuma Diffraction KM-4	Siemens P3	Kuma Diffraction KM-4	Siemens P3
Data collection method	ω–2θ scans	ω–2θ scans	ω–2θ scans	ω–2θ scans
Absorption correction	None	None	Psi-scan	None
T_{min}	–	–	0.514	–
T_{max}	–	–	0.982	–
No. of measured, independent and observed parameters	2859, 2633, 2498	4892, 3636, 2755	3067, 2274, 1761	5033, 3780, 3072
Criterion for observed reflections	$I > 2\sigma(I)$	$I > 2\sigma(I)$	$I > 2\sigma(I)$	$I > 2\sigma(I)$
R_{int}	0.0492	0.0457	0.0546	0.0165
θ_{max} (°)	30.07	30.00	74.99	27.50
Range of h, k, l	$-1 \rightarrow h \rightarrow 6$ $-1 \rightarrow k \rightarrow 13$ $-1 \rightarrow l \rightarrow 37$	$-12 \rightarrow h \rightarrow 12$ $-1 \rightarrow k \rightarrow 7$ $-1 \rightarrow l \rightarrow 36$	$-1 \rightarrow h \rightarrow 16$ $-9 \rightarrow k \rightarrow 1$ $-1 \rightarrow l \rightarrow 33$	$-11 \rightarrow h \rightarrow 11$ $-22 \rightarrow k \rightarrow 1$ $-14 \rightarrow l \rightarrow 1$
No. and frequency of standard reflections	3 every 100 reflections	3 every 97 reflections	3 every 100 reflections	3 every 97 reflections
Intensity decay (%)	2	2	20	2
Refinement				
Refinement on	F^2	F^2	F^2	F^2
$R[F^2>2\sigma(F^2)]$, $wR(F^2)$, S	0.0319, 0.0962, 1.226	0.0408, 0.1199, 1.085	0.0636, 0.1976, 1.051	0.0363, 0.1013, 0.989
No. of reflections and parameters used in refinement	2633, 211	3636, 211	2274, 217	3780, 281
H-atom treatment	All H-atom parameters refined	All H-atom parameters refined	All H-atom parameters refined	All H-atom parameters refined
Weighting scheme	$w = 1/[\sigma^2(F_o^2) + (0.0468P)^2 + 0.5406P]$, where $P = (F_o^2 + 2F_c^2)/3$	$w = 1/[\sigma^2(F_o^2) + (0.0684P)^2 + 0.0258P]$, where $P = (F_o^2 + 2F_c^2)/3$	$w = 1/[\sigma^2(F_o^2) + (0.1429P)^2 + 0.2720P]$, where $P = (F_o^2 + 2F_c^2)/3$	$w = 1/[\sigma^2(F_o^2) + (0.0577P)^2 + 0.3264P]$, where $P = (F_o^2 + 2F_c^2)/3$
$(\Delta/\sigma)_{max}$	0.027	0.004	0.011	0.001
$\Delta\rho_{max}$, $\Delta\rho_{min}$ (e Å^{-3})	0.375, −0.332	0.313, −0.289	0.334, −0.336	0.224, −0.368
Extinction method	None	None	*SHELXL*97	None
Extinction coefficient	–	–	0.0031 (6)	–

Computer programs used: *KM*-4 (Kuma Diffraction, 1991), *DATAPROC*9.0 (Gałdecki *et al.*, 1995), *SHELXS*97 (Sheldrick, 1997*b*), *SHELXL*97 (Sheldrick, 1997*a*), *P*3 (Siemens, 1989), *XDISK* (Siemens, 1991).

refinement of Flack's (1983) absolute structure parameter; its final value was −0.01 (7).

Standard bond lengths quoted throughout the paper have been taken from the *International Tables for Crystallography* (Allen *et al.*, 1992). The van der Waals radii are from Bondi (1964).

The interactive molecular graphics programs *SYBYL* (Tripos Associates Inc., 1996), *InsightII* (Molecular Simulations Inc., 1997) and *XP* (Siemens, 1990) have been used for analysis of molecular geometry and the preparation of drawings.

2.3. Molecular orbital calculations

Final molecular electronic properties have been calculated in a single point for X-ray determined coordinates. The restricted Hartree–Fock (RHF) method and the triple zeta 6-311++G(3df,2p) basis set as implemented in *Gaussian*98

Table 2
Selected geometrical parameters (Å, °).

	(Io)	(Im)	(II)	(III)
Bond lengths (Å)				
S═O1	1.437 (1)	1.433 (1)	1.425 (2)	1.439 (1)
S═O2	1.443 (1)	1.434 (1)	1.443 (3)	1.438 (1)
S—C1	1.789 (2)	1.785 (2)	1.773 (4)	1.820 (1)
S—C9	1.757 (2)	1.762 (2)	1.767 (3)	1.768 (1)
C1—C2	1.519 (3)	1.523 (2)	1.517 (5)	1.539 (2)
C1—C15	–	–	–	1.516 (2)
C2═O3	1.209 (3)	1.209 (2)	1.219 (5)	1.213 (2)
C2—C3	1.491 (3)	1.481 (4)	1.484 (5)	1.486 (2)
C12—Cl	–	–	1.730 (4)	–
Intramolecular non-bonding distances (Å), accompanied by corresponding sums of the van der Waal's radii (Å) given in square brackets				
S···O3 [3.32]	3.188 (2)	3.428 (1)	2.926 (3)	2.894 (1)
O1···C2 [3.22]	3.340 (3)	3.913 (2)	3.254 (4)	3.116 (2)
O2···C2 [3.22]	2.836 (3)	3.309 (2)	3.186 (5)	3.272 (2)
Valency and torsion angles (°)				
S—C1—C2	107.5 (1)	114.6 (1)	113.9 (3)	110.0 (1)
α: S—C1—C2—O3	−76.0 (2)	89.8 (2)	−4.1 (5)	18.7 (2)
β: O1—S—C1—C2	88.9 (1)	−158.7 (1)	70.4 (3)	60.4 (1)
β': O1—S—C1—C15	–	–	–	−175.1 (1)
γ: O2—S—C1—C2	−39.3 (2)	72.3 (1)	−60.8 (3)	−71.0 (1)
γ': O2—S—C1—C15	–	–	–	53.4 (1)

Table 3
Selected CHELPG (Breneman & Wiberg, 1990) electrostatic atomic charges (e), overall Hartree–Fock molecular energy E(HF) (H), dipole moments D_m (D), HOMO and LUMO energies (eV); all properties were calculated at the HF/6-311++G(2df,2p) level.

	(Io)	(Im)	(II)	(III)
S	1.128	1.066	1.158	1.124
O1	−0.600	−0.595	−0.592	−0.600
O2	−0.599	−0.599	−0.603	−0.598
O3	−0.529	−0.575	−0.509	−0.483
C1	−0.161	−0.097	−0.266	−0.191
H1	0.029	0.061	0.049	0.051
H2	0.076	0.065	0.061	–
C2	0.561	0.570	0.652	0.566
C3	−0.066	−0.146	−0.184	−0.079
C9	−0.164	−0.157	−0.117	−0.159
C15	–	–	–	0.158
Cl	–	–	−0.130	–
E(HF)	−1159.31555	−1159.32013	−1618.24110	−1388.81764
D_m	8.27	4.15	7.68	8.45
HOMO	−10.052	−9.814	−9.777	−9.592
LUMO	0.691	1.431	0.672	0.727

Table 4
Mayers's bond orders of selected bonds as calculated at the BLYP/DNP level.

	(Io)	(Im)	(II)	(III)
S═O1	1.89	1.88	1.92	1.89
S═O2	1.88	1.90	1.90	1.88
S—C1	1.17	1.26	1.16	1.12
S—C9	1.14	1.15	1.12	1.13
C1—C2	1.03	1.11	1.06	1.02
C1—H1	0.61	0.50	0.60	0.38
C1—H2	0.59	0.61	0.61	–
C1—C15	–	–	–	1.08
C2═O3	1.89	1.86	1.90	1.91
C2—C3	1.01	1.02	1.02	1.01
C12—Cl	–	–	1.17	–

(Frisch *et al.*, 1998) has been applied. Atomic charges were computed to fit the electrostatic potential at points selected accordingly to the high sampling CHELPG scheme (Breneman & Wiberg, 1990). Mayer's (1986) bond orders were calculated with the *DMOL* (Molecular Simulations Inc., 1996) using the density functional theory formalism (Hohenberg & Kohn, 1964; Levy, 1979). The DNP double-zeta quality basis set (equivalent to the 6-31G**) and the gradient-corrected correlation functionals BLYP (Lee *et al.*, 1988) were applied.

Natural bond orbital calculations were performed using Version 3.1 of the *NBO* program (Glendening *et al.*, 1992), as implemented in *Gaussian*98 (Frisch *et al.*, 1998). Due to the restriction of the maximum number of orbitals which can be evaluated by the *NBO* program, all natural bond analyses were performed in the 6-31G(d,p) basis.

3. Results and discussion

A view of the compounds investigated with the atom-numbering scheme is shown in Fig. 1. Relevant geometrical parameters are given in Table 2. Electrostatic-potential-derived atomic charges and selected molecular electronic properties are summarized in Table 3. Mayer's bond orders are in Table 4.

3.1. Molecular structure of (Io) and (Im)

In the crystal both polymorphs (Io) and (Im) adopt a different conformation, see Fig. 2 for comparison. The α: S—C1—C2—O3 dihedral angles in (Io) and (Im) [−76.0 (2) and 89.8 (2)°, respectively] indicate that the β-carbonyl groups are approximately *gauche* with respect to the S—C1 bonds. The S═O1 and S═O2 bonds, when referring to the central C1—C2 bonds, are either *gauche*, *gauche* [as in (Io)] or *anti*, *gauche* [as in (Im)].

The electrostatic-potential-derived atomic charge distribution is quite similar in both polymorphs. All O atoms bear substantial negative atomic charges, while the S and C2 atoms are positively charged. This charge arrangement favours electrostatic interactions between the oppositely charged atoms of the S═O and C═O bonds. Indeed, the conformation of the unstable orthorhombic (Io) polymorph is controlled by two cross, intramolecular S···O3 and C2···O2 contacts which are significantly shorter [3.188 (2) and 2.836 (3) Å, respectively] than the respective sums of the van der Waals radii (3.32 and 3.22 Å). During the daylight-induced polymorphic transformation from (Io) to the more stable (Im), these distances have undergone significant elongation [to 3.428 (1) and 3.309 (2) Å, respectively] and are extended out of the van der Waals limits. The S—C1—C2 valency angle defined around the pivotal C1 atom is more restricted in (Io) [107.5 (1) Å] than in (Im) [114.6 (1) Å] and indicates the more relaxed conformation of the latter polymorph. Negative charges are located on the C1 atoms (−0.161 and −0.097 e, respectively), while the methylene H1 and H2 atoms are positively charged. The C1—H1 and C1—H2 Mayer's bond

orders [0.61, 0.59 and 0.50, 0.61 for (Io) and (Im), respectively] are much smaller than unity, indicating weak bonds which are prone to electrolytic dissociation. This conclusion is in good agreement with the earlier experimental observations which had shown that in the ethanol solution benzoylmethyl phenyl sulfones exhibit acid properties. Amel & Marek (1973) had suggested that in the resulting carboanion (IV)

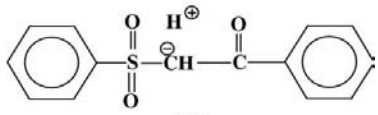

(IV)

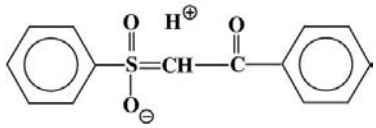

(V)

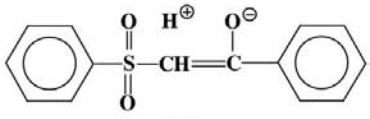

(VI)

the negative charge formally located on a methylene C1 atom is redistributed to the sulfonyl and carbonyl O atoms in a fashion illustrated by the resonance structures similar to (V) and (VI).

The dipole moment of the (Im) molecule is much lower than that of (Io) (4.15 and 8.27 D, respectively). As already mentioned above, in (Io) the C1 negative charge is larger than in (Im). The S—C1 and C1—C2 Mayer's bond orders in (Im) (1.26 and 1.11, respectively) are larger than in (Io) (1.17 and 1.03, respectively). The carbonyl C2═O3 bond order in (Im) (1.86) is slightly smaller than that in (Io) (1.89). No similar simple relation is observed for the sulfonyl S═O bonds. The latter bonds exhibit pronounced dipolar character (Oae, 1985) and therefore their Mayer's bond orders are less prone to changes resulting from the electron density variations (Wolf, 2001). The above simple comparison indicates that the firm (Im) polymorph is to a larger extent than (Io) stabilized by the electron density delocalizations as described by structures (IV) and (V). Comparison of the overall molecular SCF energy, as calculated at the HF/6-311++G(2df,2p) level shows that the energy of (Im) is only 12.14 kJ mol^{-1} lower than that of (Io).

Crystal packing diagrams of both polymorphs (Io) and (Im) are presented in Fig. 3. Intermolecular distances slightly shorter than the respective van der Waals limits involve methylene H1 and H2 and O atoms (details are summarized in Table 5). According to a liberal definition of Desiraju & Steiner (1999) these contacts can be classified as very weak hydrogen bonds. The observed polymorphic transformation introduces significant changes to the overall crystal symmetry (from $P2_12_12_1$ to $P2_1/c$). If no bonds had been broken during the transformation it would have required large translations and rotations of entire molecules in the crystal. Detailed analysis of the crystal packing shows that in the crystal there is no ample space for such complex movements. Furthermore, long and complicated motions are unlikely because they would have generated high tensions which could eventually destroy the crystal. Therefore, the mechanism of the observed transformation is presumably based on the initial photochemical cleavage of the S—C1 bonds. The resulting free radicals migrate in the crystal and further recombine to give the stable polymorph (Im). The free radical S—C1 bond splitting has often been observed during the photodegradation of benzoylmethyl phenyl sulfones (Wagner & Lindstrom, 1987). The photochemical origin of the above described polymorphic transformation is additionally supported by the fact that this reaction does not proceed without the presence of daylight.

3.2. Molecular structure of (II) and (III)

In the crystal both compounds (II) and (III) adopt an extended conformation, see Fig. 4 for a comparison. The central S—C1 bonds are positioned *syn* when related to the *β*-

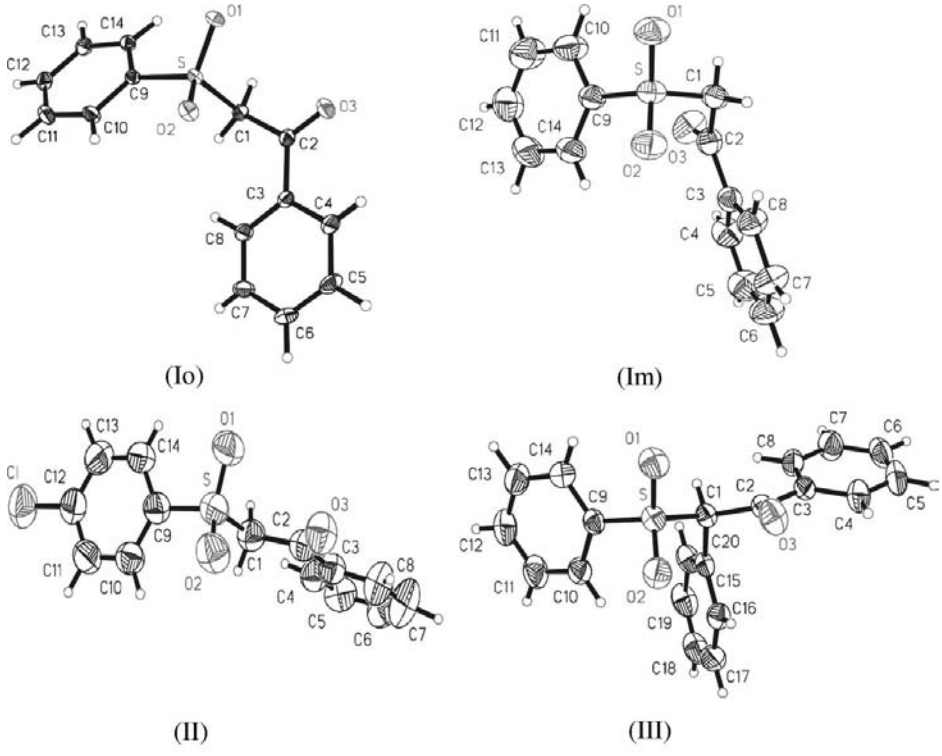

Figure 1
View of investigated compounds. Thermal ellipsoids were drawn at the 50% probability level.

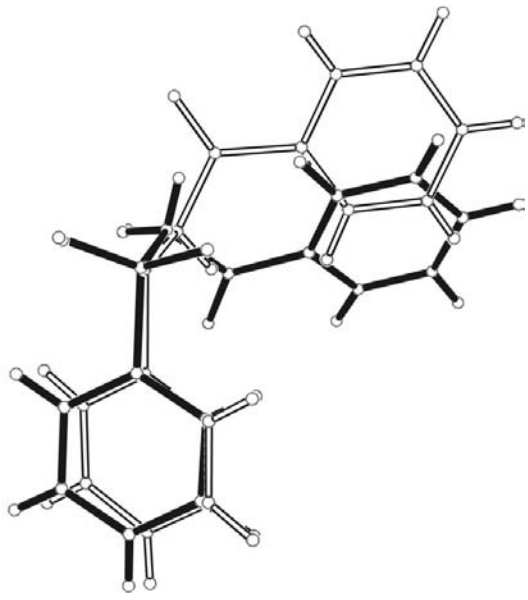

Figure 2
Superposition of (Io) and (Im) polymorphs as indicated by empty and solid lines, respectively. Both conformations were plotted using atom coordinates determined by an X-ray crystallography. The least-squares fit was based on S, O1, O2, C1, C2, C9, C10, C11, C12, C13 and C14 atoms, and the root mean-square deviation was 0.12 Å.

carbonyl group, while the sulfonyl S═O1 and S═O2 bonds are both *gauche* with respect to the C1—C2 bonds.

The atomic charge arrangement is similar to that observed in the previously discussed polymorphs (Io) and (Im). The S—C1 bond in the X-ray determined structure of (III) is more stretched [1.820 (1) Å] than the normally observed S—C single bond 1.78 Å. It is also longer than the corresponding bonds in (Io), (Im) and (II) [1.789 (2), 1.785 (2) and 1.773 (4) Å, respectively]. Furthermore, comparison of the non-bonding distances clearly shows that steric repulsions like those described by Rûchardt & Beckhaus (1985) cannot be a major reason for the S—C1 bond elongation in (III). The S—C1 and C1—C2 bond orders in (II) (1.16 and 1.06, respectively) and (III) (1.12 and 1.02, respectively) are smaller than their analogues observed in the stable polymorph (Im) (1.26 and 1.11, respectively). This simple analysis suggests that the electron density delocalizations in (II) and especially in (III) are less intensive than in (Im). Examination of the relevant intramolecular distances summarized in Table 2 shows that interactions between the oppositely charged S and O3 atoms are stronger in (II) and (III) than in (Io). On the other hand, the O2···C2 attraction is stronger in (Io).

Crystal packing diagrams of compounds (II) and (III) are presented in Fig. 5. As in previously characterized crystals of (Io) and (Im), very weak intermolecular hydrogen bonds link H atoms at the pivotal C1 atoms with the sulfonyl group O atoms.

3.3. Hyperconjugative interactions

In addition to the already characterized, intramolecular, electrostatic attraction between the oppositely charged atoms of the sulfonyl and carbonyl groups, conformation of β-ketosulfones is often influenced by the mutual hyperconjugative (Hoffmann, 1971) σ^*(S—C1) $-$ π(C2═O3) and σ(S—C1) $-$ π^*(C2═O3) interactions. In particular, these effects were identified by Distefano *et al.* (1991, 1996) and Dal Colle *et al.* (1995) to be responsible for the predominant *gauche* conformation of the central S—C1—C2═O3 fragment, as found in several β-benzoylmethyl phenyl sulfones (Gałdecka & Gałdecki, 1999; Grossert *et al.*, 1988; Kokkou & Cheer, 1986; Krawiec *et al.*, 1989). In the present work, calculations of the hyperconjugative stabilization energies in (Io), (Im), (II) and (III) were performed using Weinhold's *et al.* natural bond

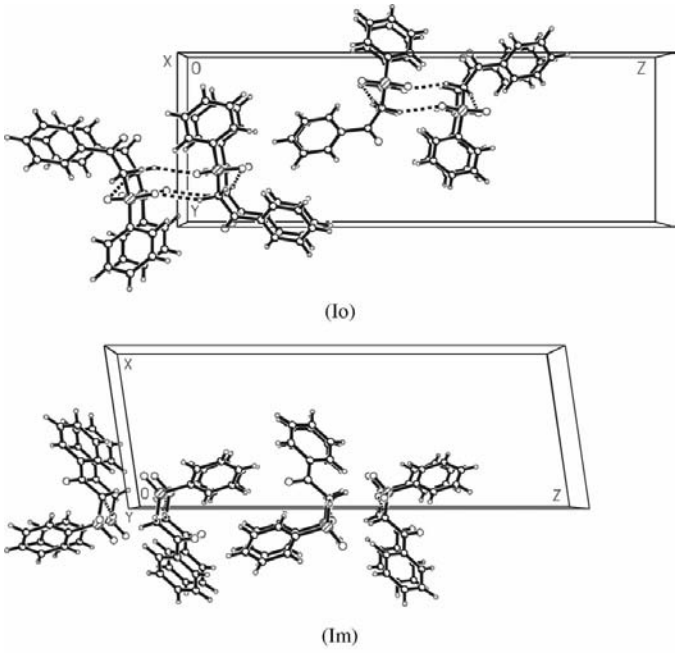

Figure 3
Perspective drawings of the (Io) and (Im) crystal structures viewed parallel to the *a* and *b* axes, respectively. Very weak hydrogen bonds are indicated with dashed lines.

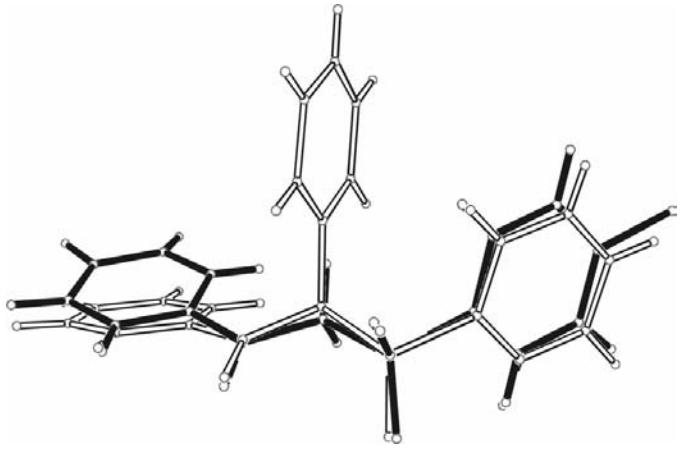

Figure 4
Superposition of (II) and (III) molecules as determined by an X-ray analysis. The least-squares fit was based on S, O1, O2, O3, C1, C2, C3 and C9 atoms, the root mean-square deviation was 0.17 Å.

Table 5
Hydrogen-bonding geometry (Å, °) for (Io), (Im), (II) and (III).

D—H···A	D—H	H···A	D···A	< (D—H···A)
(Io)				
C1—H1···O2^{i}	0.99 (2)	2.44 (2)	3.413 (2)	170 (2)
C1—H2···O1^{ii}	1.02 (3)	2.38 (3)	3.347 (3)	158 (2)
(Im)				
C1—H2···O2^{iii}	0.91 (2)	2.38 (2)	3.282 (2)	170 (2)
(II)				
C1—H1···O2^{iv}	0.99 (3)	2.27 (3)	3.247 (5)	169 (2)
C1—H2···O1^{v}	1.00 (5)	2.32 (5)	3.280 (5)	161 (4)
(III)				
C1—H1···O2^{vi}	0.95 (2)	2.45 (2)	3.398 (2)	170 (2)

Symmetry codes: (i) $1+x, y, z$; (ii) $\frac{1}{2}+x, \frac{3}{2}-y, -z$; (iii) $x, 1+y, z$; (iv) $\frac{3}{2}-x, -\frac{1}{2}+y, z$; (v) $2-x, -\frac{1}{2}+y, \frac{1}{2}-z$; (vi) $x, \frac{1}{2}-y, \frac{1}{2}+z$.

orbital (NBO) analysis of the Hartree–Fock wavefunctions (Reed *et al.*, 1988). The NBO deletion procedure (Glendening *et al.*, 1992; Reed & Schleyer, 1987; Salzner & Schleyer, 1993) was applied. Results of these calculations are summarized in Table 6.

The σ(S—C1) − π^*(C2═O3) stabilization in (Io) is slightly larger than that in (Im), while the reverse back-donation σ^*(S—C1) − π(C2═O3) is weaker. It means that as compared to (Im), in (Io) more electron density is transferred from S—C1 towards the C2═O3 bond. Consequently, in (Io) the former bond becomes weaker and the latter becomes stronger. Very small σ(S—C1) − π^*(C2═O3) and σ^*(S—C1) − π(C2═O3) stabilization energies in (II) and (III) follow from the *synperiplanar* arrangement of the S—C1 and C2═O3 bonds. The intensities of these interactions in benzoylmethyl phenyl sulfones are highly dependent on α, *i.e.* the central S—C1—C2—O3 dihedral angle. This relationship is clearly visible in Fig. 6. The σ(S—C1) − π^*(C2═O3) and σ^*(S—C1) − π(C2═O3) stabilization energies, calculated for the systematic α scans and (Im) as a starting conformer, reached the highest values at two α torsion angles −105 and 105°, respectively. For the *synperiplanar* rotamer hyperconjugative stabilization energies are close to zero. These results are consistent with the general observation that the anomeric effect is the most effective when interacting polar bonds are positioned *gauche* with respect to each other (Graczyk & Mikołajczyk, 1994; Juaristi & Cuevas, 1995, and references therein). The so-called *syn*-anomeric effect (Irwin *et al.*, 1990) plays only a marginal role in the investigated compounds (II) and (III).

Electron density distribution in (Io), (Im), (II) and (III) is significantly affected by interactions of the oxygen lone pairs with non-bonding orbitals of the adjacent S—C1 and C1—C2 bonds. The resulting stabilization energies are summarized in Table 6. Contradictory to the previously analysed σ^*(S—C1) − π(C2═O3) and σ(S—C1) − π^*(C2═O3) hyperconjugation, the intensity of these interactions is similar in all investigated compounds and does not significantly depend on the α dihedral angle. See Fig. 7 for a comparison. This effect is to a

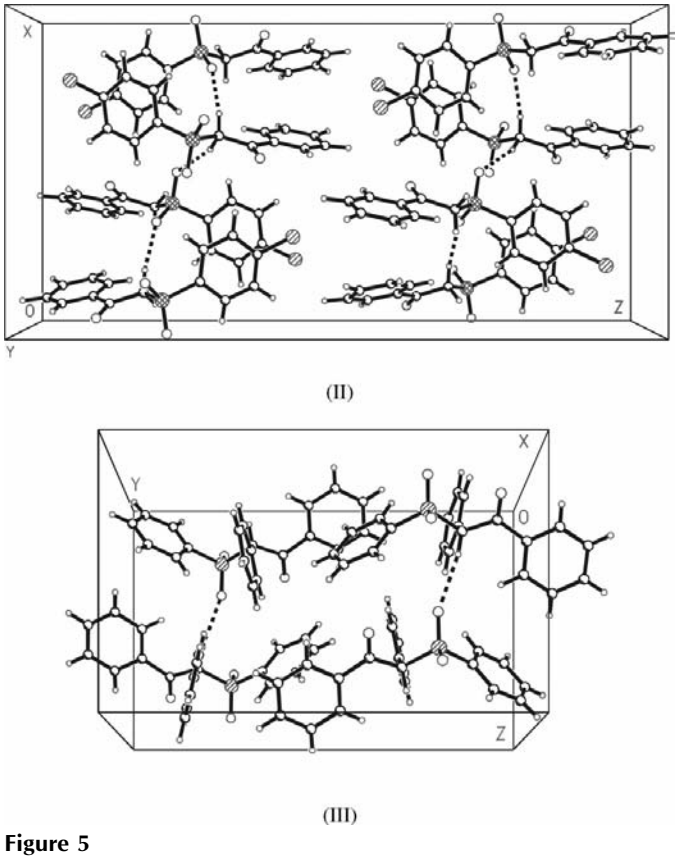

Figure 5
Perspective drawings of the (II) and (III) crystal structures viewed parallel to the *b* and *a* axes, respectively. Hydrogen bonds are indicated with dashed lines.

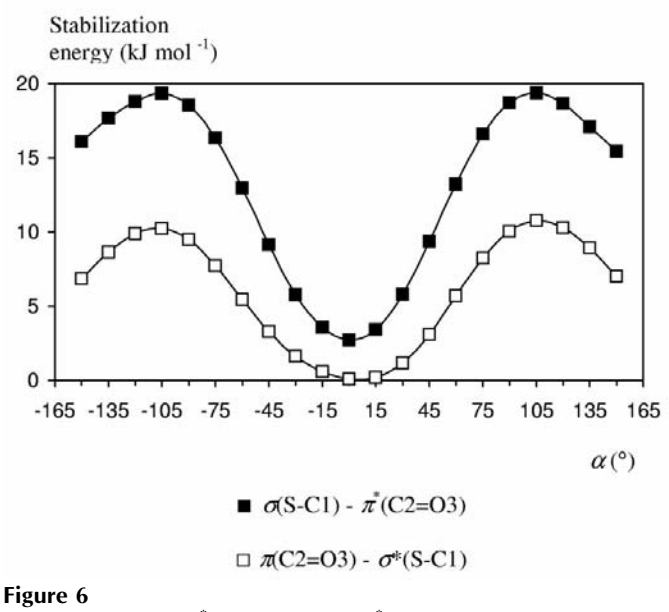

Figure 6
The σ(S—C1) − π^*(C2═O3) and σ^*(S—C1) − π(C2═O3) NBO stabilization energies (kJ mol^{-1}) plotted as a function of α: S—C1—C2═O3 dihedral angle (°). Energies were calculated for the systematic α scans ($\Delta\alpha$ = ±15°) and the X-ray structure of (Im) as a starting conformer. Due to severe steric clashes of the terminal phenyl rings, only $-150 \leq \alpha \leq 150$ values were allowed.

Table 6
The NBO stabilization energies in (kJ mol^{-1}) of the selected pairs of the bonding and non-bonding natural orbitals, as calculated with the natural bond orbital deletion procedure (Glendening *et al.*, 1992).

Non-bonding orbitals are indicated by stars. The symbol n(O1,O2) represents the natural orbitals defining lone pairs of the sulfonyl group O1 and O2 atoms; n(O3) represents the related orbitals of the carbonyl group O3 atom.

	σ(S—C1) − π^*(C2═O3)	σ^*(S—C1) − π(C2═O3)	n(O1,O2) − σ^*(S—C1)	n(O3) − σ^*(S—C1)
(Io)	21.256	6.624	170.650	96.083
(Im)	18.669	10.053	165.739	93.562
(II)	1.402	0.201	174.677	97.477
(III)	2.031	0.251	175.171	97.636

large extent responsible for back-donation of the electron density from the O atoms towards the central part of a molecule. It partially counteracts the strongly electron-withdrawing character of the benzoylmethyl and especially phenylsulfonyl moieties, as confirmed by highly positive values of their Hammett's σ_p constants 0.43 and 0.70, respectively (Hansch & Leo, 1979).

The nature of the S atom electron density back-donation has been a matter of controversy over a long period of time. Traditional interpretation assumed overlapping of the sulfur non-bonding *d* orbitals with π orbitals of the adjacent bonds (Kwart & King, 1977, and references therein). In (Io), (Im), (II) and (III) the natural population analysis (NPA) calculated within the NBO framework showed that *d* orbitals participate in hybrids describing the electronic configurations of S atoms for all bonds of the sulfur coordination sphere in less than 3%. Their contribution to the overall stabilization energy was close to zero. Therefore, the S atom electron density back-donation is mostly realised through the n(O1,O2) − σ^*(S—C1) and n(O3) − σ^*(S—C1) interactions and proceeds without significant involvement of the non-bonding sulfur *d* orbitals.

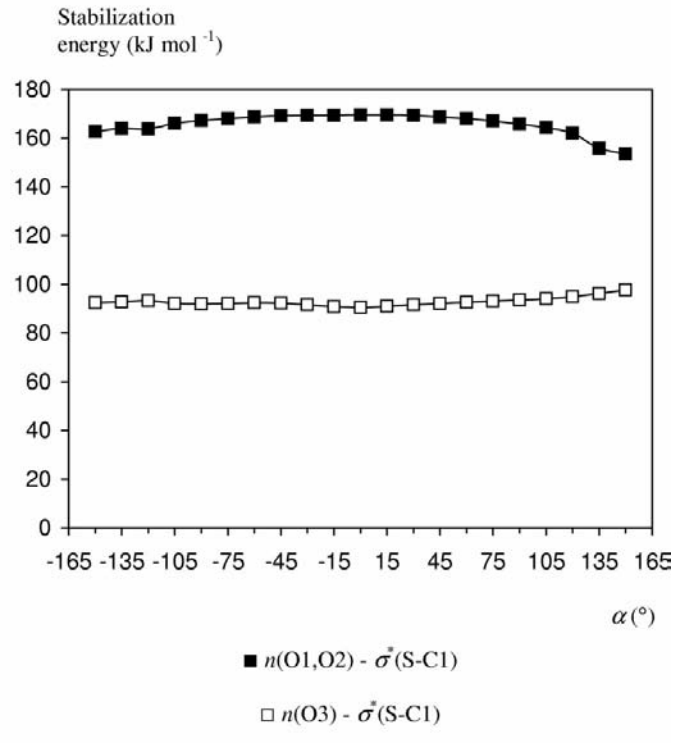

Figure 7
The n(O1,O2) − σ^*(S—C1) and n(O3) − σ^*(S—C1) NBO stabilization energies (kJ mol^{-1}) plotted as a function of α: S—C1—C2═O3 dihedral angle (°). Energies were calculated in the same way as described in the legend to Fig. 6. The n(O1,O2) and n(O3) symbols are the same as characterized in Table 6.

4. Conclusions

In all the compounds investigated, (Io), (Im), (II) and (III), the electron density distribution favours electrostatic attraction between the oppositely charged atoms of the S═O and C═O bonds. These interactions constrain the conformations of (Io), (II) and (III) by contracting the S···O3 and C2···O2 intramolecular distances below the respective van der Waals limits. However, the restrained conformation of the fragile orthorhombic polymorph (Io) is relieved during the light-induced solid-state transformation which finally gives the stable monoclinic crystals of (Im). Conformation of the latter polymorph is to a larger extent than (Io) stabilized by the electron density delocalizations.

Hyperconjugative σ(S—C1) − π^*(C2═O3) and σ^*(S—C1) − π(C2═O3) stabilization energies in benzoylmethyl phenyl sulfones are highly dependent on α: S—C1—C2═O3 (central dihedral angle) and are largest for the *gauche* arrangement, as found in (Io) and (Im). For the *synperiplanar* conformation [as in (II) and (III)] these energies are approaching zero. The electron density distribution in all compounds (Io), (Im), (II) and (III) is significantly affected by interactions of the oxygen lone pairs with non-bonding orbitals of the adjacent S—C1 and C1—C2 bonds. This effect is responsible for back-donation of the electron density from the O atoms towards the central part of a molecule and counteracts the strongly electron-withdrawing character of the benzoylmethyl and especially phenylsulfonyl moieties.

The author is indebted to Dr Andrzej Zakrzewski (Technical and Agricultural Academy, Bydgoszcz, Poland) for his valuable comments and samples of (I)–(III). Quantum chemical calculations were performed in the ACK CYFRONET, Kraków, Poland; support through computational grants 030/1999 and 050/1999 is gratefully acknowledged.

References

Allen, F. H. & Kennard, O. (1993). *Chem. Des. Autom. News*, **8**, 31–37.

Allen, F. H., Kennard, O., Watson, D. G., Brammer, L., Orpen, A. G. & Taylor, R. (1992). *International Tables for Crystallography*, Vol. C, edited by A. J. C. Wilson, pp. 691–705. Dordrecht: Kluwer Academic Publishers.
Amel, R. T. & Marek, P. J. (1973). *J. Org. Chem.* **38**, 3513–3516.
Bondi, A. (1964). *J. Phys. Chem.* **68**, 441–451.
Borchardt, A., Kopkowski, A., Kornacki, Z. & Zakrzewski, A. (1990). *J. Chem. Soc. Perkin Trans. 2*, pp. 845–848.
Borchardt, A., Kopkowski, A., Wasilewski, W. & Zakrzewski, A. (1990). *Bydgoskie Tow. Nauk. Prace Wydz. Nauk. Techn. A*, **18**, 35–41.
Breneman, C. M. & Wiberg, K. B. (1990). *J. Comput. Chem.* **11**, 361–373.
Dal Colle, M., Bertolasi, V., de Palo, M., Distefano, G., Jones, D., Modelli, A. & Olivato, P. R. (1995). *J. Phys. Chem.* **99**, 15011–15017.
Desiraju, G. R. & Steiner, T. (1999). *The Weak Hydrogen Bond*, p. 44. New York: Oxford University Press.
Distefano, G., Dal Colle, M., Bertolasi, V., Olivato, P. R., Bonfada, É. & Mondino, M. G. (1991). *J. Chem. Soc. Perkin Trans. 2*, pp. 1195–1199.
Distefano, G., Dal Colle, M., de Palo, M., Jones, D., Bombieri, G., Del Pra, A., Olivato, P. R. & Mondino, M. G. (1996). *J. Chem. Soc. Perkin Trans. 2*, pp. 1661–1669.
Drabik, J., Piotrowski, W. & Zakrzewski, A. (1990). *Bydgoskie Tow. Nauk. Prace Wydz. Nauk. Techn. A*, **18**, 16–23.
Flack, H. D. (1983). *Acta Cryst.* A**39**, 876–881.
Frisch, M. J., Trucks, G. W., Schlegel, H. B., Scuseria, G. E., Robb, M. A., Cheeseman, J. R., Zakrzewski, V. G., Montgomery Jr, J. A., Stratmann, R. E., Burant, J. C., Dappich, S., Millam, J. M., Daniels, A. D., Kudin, K. N., Strain, M. C., Farkas, O., Tomasi, J., Barone, V., Cossi, M., Cammi, R., Mennucci, B., Pomelli, C., Adamo, C., Clifford, S., Ochterski, J., Petersson, G. A., Ayala, P. Y., Cui, Q, Morokuma, K., Malick, D. K., Rabuck, A. D., Raghavachari, K., Foresman, J. B., Ciosłowski, J., Ortiz, J. V., Stefanov, B. B., Liu, G., Liashenko, A., Piskorz, P., Komaromi, I., Gomperts, R., Martin, R. L., Fox, D. J., Keith, T., Al-Laham, M. A., Peng, C. Y., Nanayakkara, A., Gonzalez, C., Challacombe, M., Gill, O. M. W., Johnson, B. G., Chen, W., Wong, J. L., Andres, J. L., Head-Gordon, M., Replogle, E. S. & Pople, J. A. (1998). *Gaussian*98. Revision A.6. Gaussian Inc., Pittsburgh PA, USA.
Gałdecka, E. & Gałdecki, Z. (1999). *Pol. J. Chem.* **73**, 821–843.
Gałdecki, Z., Kowalski, A. & Uszyński, L. (1995). *DATAPROC*, Version 9.0. Kuma Diffraction, Wrocław, Poland.
Glendening, E. D., Reed, A. E., Carpenter, J. E. & Weinhold, F. (1992). *NBO Program Manual*. University of Wisconsin, USA.
Graczyk, P. R. & Mikołajczyk, M. (1994). *Topics in Stereochemistry*, edited by E. L. Eliel and S. H. Wilen, Vol. 21, pp. 159–349. New York: Wiley.
Grossert, J. S., Ranjith, H., Dharmaratne, T., Cameron, T. S. & Vincent, B. R. (1988). *Can. J. Chem.* **66**, 2860–2869.
Hansch, C. & Leo, A. (1979). *Substituents Constants for the Correlation Analysis in Chemistry and Biology*. Weinheim: Verlag Chemie.
Hoffmann, R. (1971). *Acc. Chem. Res.* **4**, 1–9.
Hohenberg, P. & Kohn, W. (1964). *Phys. Rev. B*, **136**, 864–871.
Irwin, J. J., Tae-Kyu, H. & Dunitz, J. D. (1990). *Helv. Chim. Acta*, **73**, 1805–1817.
Juaristi, E. & Cuevas, G. (1995). *New Directions in Organic and Biological Chemistry*, edited by C. W. Reeds, p. 31. Boca Raton: CRC Press.
Kokkou, S. C. & Cheer, C. J. (1986). *Acta Cryst.* C**42**, 1074–1076.
Krawiec, M., Krygowski, T. M. & Zakrzewski, A. (1989). *Acta Cryst.* C**45**, 345–346.
Kuma Diffraction (1991). *KM*-4 *User's Guide*, Version 3.2. Kuma Diffraction, Wrocław, Poland.
Kwart, H. & King, K. (1977). *d-Orbitals in the Chemistry of Silicon, Phosphorus and Sulfur.* Berlin: Springer.
Lee, C., Yang, W. & Parr, R. G. (1988). *Phys. Rev. B*, **37**, 785–789.
Levy, M. (1979). *Proc. Natl. Acad. Sci. USA*, **76**, 6062–6065.
Mayer, I. (1986). *Int. J. Quantum Chem.* **29**, 477–483.
Molecular Simulations Inc. (1996). *DMOL User's Guide*, Version 96.0. Molecular Simulations Inc., San Diego, USA.
Molecular Simulations Inc. (1997). *Insight*II *User's Guide*, Version 4.0.0. Molecular Simulations Inc., San Diego, USA.
Oae, S. (1985). *Organic Sulfur Chemistry. Theoretical and Experimental Advances*, edited by F. Bernardi, I. G. Csizmadia and A. Mangini, pp. 1–67. Amsterdam: Elsevier.
Olivato, P. R., Guerrero, S. A. & Zukerman-Schpector, J. (2000). *Acta Cryst.* B**56**, 112–117.
Olivato, P. R., Mondino, M. G., Yreijo, M. H., Blanka, W., Bjorklund, M. B., Marzorati, L., Distefano, G., Dal Colle, M., Bombieri, G. & Del Pra, A. (1998). *J. Chem. Soc. Perkin Trans. 2*, pp. 109–114.
Reed, A. E., Curtiss, L. A. & Weinhold, F. (1988). *Chem. Rev.* **88**, 899–926.
Reed, A. E. & Schleyer, P. v. R. (1987). *J. Am. Chem. Soc.* **109**, 7362–7373.
Rûchardt, Ch. & Beckhaus, H.-D. (1985). *Angew. Chem. Int. Ed. Engl.* **24**, 529–538.
Salzner, U. & Schleyer, P. v. R. (1993). *J. Am. Chem. Soc.* **115**, 10231–10236.
Sheldrick, G. M. (1997*a*). *SHELXL*97. University of Göttingen, Germany.
Sheldrick, G. M. (1997*b*). *SHELXS*97. University of Göttingen, Germany.
Siemens (1989). *P*3, Version 2.0. Siemens Analytical X-ray Instruments Inc., Madison, Wisconsin, USA.
Siemens (1990). *XP*, Version 4.1. Siemens Analytical X-ray Instruments Inc., Madison, Wisconsin, USA.
Siemens (1991). *XDISK*, Version 4.20. Siemens Analytical X-ray Instruments Inc., Madison, Wisconsin, USA.
Tripos Associates Inc. (1996). *SYBYL*, Version 6.3. Tripos Associates Inc., St Louis, Missouri, USA.
Wagner, P. J. & Lindstrom, M. J. (1987). *J. Am. Chem. Soc.* **109**, 3062–3067.
Wolf, W. M. (1999*a*). *Acta Cryst.* C**55**, 469–472.
Wolf, W. M. (1999*b*). *J. Mol. Struct.* **474**, 113–124.
Wolf, W. M. (2000). *Acta Cryst.* C**56**, 1444–1446.
Wolf, W. M. (2001). *Acta Cryst.* B**57**, 54–62.
Zakrzewski, A. (1999). *Przem. Chem.* **78**, 17–19.
Zakrzewski, A. & Kacała, A. (1998). *Pestycydy*, **4**, 21–30.